Interhemispheric plasticity is mediated by maximal potentiation of callosal inputs

Emily Petrus[a,1], Galit Saar[a], Zhiwei Ma[a], Steve Dodd[a], John T. R. Isaac[b], and Alan P. Koretsky[a,1]

[a]Laboratory of Functional and Molecular Imaging, National Institute of Neurological Disorders and Stroke, National Institutes of Health, Bethesda, MD 20892; and [b]Department of Physiology, University of Toronto, Toronto ON MS5 1A8, Canada

Edited by Marcus E. Raichle, Washington University in St. Louis, St. Louis, MO, and approved February 6, 2019 (received for review June 14, 2018)

Central or peripheral injury causes reorganization of the brain's connections and functions. A striking change observed after unilateral stroke or amputation is a recruitment of bilateral cortical responses to sensation or movement of the unaffected peripheral area. The mechanisms underlying this phenomenon are described in a mouse model of unilateral whisker deprivation. Stimulation of intact whiskers yields a bilateral blood-oxygen-level–dependent fMRI response in somatosensory barrel cortex. Whole-cell electrophysiology demonstrated that the intact barrel cortex selectively strengthens callosal synapses to layer 5 neurons in the deprived cortex. These synapses have larger AMPA receptor- and NMDA receptor-mediated events. These factors contribute to a maximally potentiated callosal synapse. This potentiation occludes long-term potentiation, which could be rescued, to some extent, with prior long-term depression induction. Excitability and excitation/inhibition balance were altered in a manner consistent with cell-specific callosal changes and support a shift in the overall state of the cortex. This is a demonstration of a cell-specific, synaptic mechanism underlying interhemispheric cortical reorganization.

corpus callosum | cortical circuit | interhemispheric plasticity

The brain has an amazing capacity to adapt to perturbations in peripheral or central nervous systems. For example, a left hemisphere stroke in human language areas often results in aphasia: the loss of language. The right hemisphere's recruitment is associated with better language recovery (1), while further damage to the right hemisphere worsens aphasia symptoms (2). Humans with a unilateral stroke in somatosensory/motor areas demonstrate widespread changes in blood-oxygen-level–dependent (BOLD) fMRI signal during unaffected hand motions (3), with bilateral activation observed in patients with severe motor impairments (4). Together, these results indicate that there can be large changes in bilateral cortical responses after unilateral perturbations, which may be either beneficial or impede recovery. The cellular and synaptic changes underlying these large-scale interhemispheric circuit alterations are not defined.

Unilateral injury modifies the way contralateral homotopic cortical areas communicate via the corpus callosum (CC). The CC is required for integrating bilateral sensory signals (5), and suppresses the cortex ipsilateral to stimulation, which may enhance stimulation detection and discrimination (6). Most callosal synapses are glutamatergic and target layers 2 and 3 (L2/3) and layer 5 (L5) principal cells and interneurons (7, 8).

Unilateral infraorbital nerve (ION) transection yields a recruitment of the deprived primary somatosensory barrel cortex (S1BC) to ipsilateral, intact whisker stimulation, resulting in a bilateral S1BC BOLD fMRI activation (9). The recruitment of deprived S1BC relies on the presence of intact S1BC, without which the deprived S1BC is colonized by forepaw and nose responsive areas (10). In the present work, slice electrophysiology and optogenetics were used to describe the mechanism underlying the CC's targeting of deprived S1BC. The intact S1BC selectively targets L5 pyramidal neurons via the CC to alter deprived S1BC circuitry. Stronger AMPA receptor (AMPAR)-mediated activation from the CC synapse to L5 cells was detected, with a concurrent increase in NMDA receptor (NMDAR) activation. L5 neurons in deprived S1BC experience larger spontaneous excitatory events and an increase in excitability. Finally, long-term potentiation (LTP) along the CC is occluded but can be rescued following long-term depression (LTD). Together, these changes indicate a shift in the state of the deprived cortex which may enhance its response to callosal inputs. This work lays down a cellular and synaptic basis for callosal plasticity.

Results

ION Transection Produces a Bilateral S1BC BOLD fMRI Response. Mice underwent a unilateral ION transection and were imaged in an 11.7-T MRI (schematic in Fig. 1*A*). The intact S1BC demonstrated an increased response to contralateral whisker stimulation, and a recruitment of stimulus evoked fMRI BOLD response in deprived S1BC (Fig. 1 *B* and *C*, bar graph; ANOVA: $P < 0.0001$, $F = 21.3$). Incidence maps quantified the likelihood of each voxel's response. While a reliable contralateral response in sham and ION-transected animals was detected, ipsilateral activation occurred more frequently in ION-transected animals (Fig. 1*B*, *Bottom Left*). A subset of specimens was imaged postmortem in a 14-T MRI scanner to verify complete ION transection and lack of nerve regrowth (Fig. 1*D*). The increased intact S1BC BOLD response was associated with a stronger thalamocortical synaptic connection between the intact ventral posteromedial nucleus (VPM) and intact S1BC (*SI Appendix*, Fig. S1*B* and Table S1). Synaptic strength was measured by injecting a virus encoding channel rhodoposin (ChR2) into the VPM and performing whole-cell slice electrophysiology in layer 4

Significance

The corpus callosum is a large fiber bundle which connects contralateral brain regions. After unilateral perturbations such as stroke or amputation, interhemispheric connectivity is altered and often leads to bilateral somatomotor cortical hyperactivity in patients with poor recovery. This study reports that callosal targeting of deprived layer 5 neurons is maximally potentiated in mouse primary somatosensory barrel cortex after unilateral whisker denervation. These neurons also experience an increase in excitability and spontaneous excitatory amplitudes. These results should be relevant to the cortical responses observed in human patients after unilateral nerve transection, amputation, or stroke.

Author contributions: E.P., S.D., J.T.R.I., and A.P.K. designed research; E.P., G.S., and S.D. performed research; E.P., Z.M., and S.D. analyzed data; and E.P., J.T.R.I., and A.P.K. wrote the paper.

The authors declare no conflict of interest.

This article is a PNAS Direct Submission.

[1]To whom correspondence may be addressed. Email: emily.petrus@nih.gov or KoretskyA@ninds.nih.gov.

This article contains supporting information online at www.pnas.org/lookup/suppl/doi:10.1073/pnas.1810132116/-/DCSupplemental.

Published online March 7, 2019.

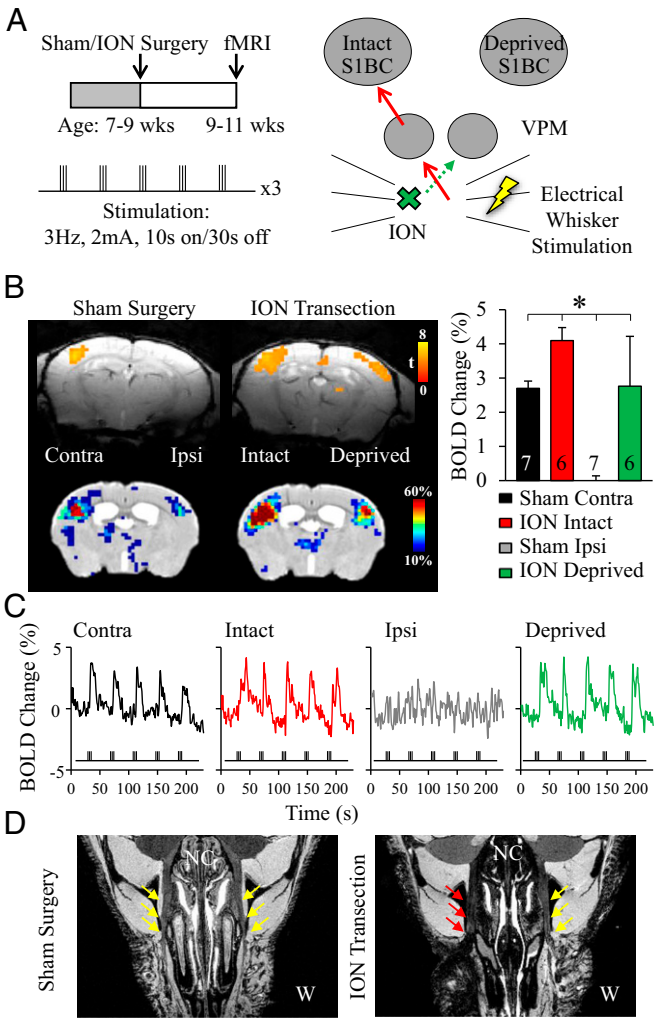

Fig. 1. Bilateral S1BC BOLD fMRI response to intact whisker stimulation. (*A*) Experimental setup. (*B*) Representative activation maps (*Top Left*). Bar graph depicts the average response amplitudes (*Right*); error bars are SEM; * denotes statistical significance. *n*, number of animals. Incidence maps depict the likelihood of each voxel's response (*Bottom Left*). (*C*) Representative traces. (*D*) Representative axial images of sham and ION transection mice. NC, nasal cavity; W, whisker pad; yellow arrows delineate ION; note the black space on ION transection animal (red arrows).

(L4) of S1BC (*SI Appendix*, Fig. S1*A*). AMPAR-mediated responses to light (LED) stimulation were isolated by substituting strontium for calcium in the artificial cerebrospinal fluid, which desynchronizes vesicle release and enables quantification of synaptic strength (11). The amplitude of strontium-evoked miniature excitatory postsynaptic currents (Sr-mEPSCs) was quantified as previously described (12). No change in synaptic strength was detected between the deprived VPM and L4 of deprived S1BC (*SI Appendix*, Fig. S1*C* and Table S1), nor were there detectible connections between intact VPM and L4 of deprived S1BC (*SI Appendix*, Fig. S1*D* and Table S1).

Bilateral task-induced fMRI response may also indicate a change in resting state connectivity. Seed-based correlation maps of S1BC were produced using nonstimulation scans. Bilateral connectivity between S1BCs was observed in sham (*SI Appendix*, Fig. S2*A*) and ION-transected (*SI Appendix*, Fig. S2*B*) mice. No difference in resting state connectivity was observed between groups (Student's *t* test: $P = 0.26$; *SI Appendix*, Fig. S2*C*).

Selective Strengthening of Callosal Synapses to L5 Principal Neurons in Deprived S1BC. We next sought to identify the synaptic locus of changes occurring in deprived S1BC which responds to intact, ipsilateral whisker stimulation. The same ChR2 virus was injected into intact S1BC and neurons in L2/3 and L5 of deprived S1BC were patched for recording (Fig. 2*A*). No change was observed in callosal strength to L2/3 neurons (Student's *t* test: $P = 0.94$; Fig. 2*B* and *SI Appendix*, Table S2). Deprived L5 neurons experience an increase in strength from callosal inputs; L5a and L5b were recorded in equal proportions (Student's *t* test: $P = 0.0006$; Fig. 2*C* and *SI Appendix*, Table S2). There was no difference in the connection probability of neurons in L2/3 or L5 responding to callosal stimulation between groups (*SI Appendix*, Fig. S3). Local L5 to L5 electrical stimulation did not detect different Sr-mEPSC amplitudes between groups (Student's *t* test: $P = 0.15$; Fig. 2*D* and *SI Appendix*, Table S3). Callosal connections are reciprocal; therefore we tested whether there were changes from deprived to intact S1BC. We measured Sr-mEPSC amplitudes from deprived to intact S1BC but did not observe a change in evoked AMPAR-mediated amplitudes (*SI Appendix*, Fig. S4*A* and Table S4). This demonstrates that the plasticity is likely unidirectional: from intact to deprived S1BC.

NMDAR Matches AMPA and Ifenprodil Sensitivity Increases at Callosally Targeted Deprived L5 Neurons. Deprived L5 neurons experience increased amplitudes of AMPAR-mediated callosal responses. Because NMDARs are also involved in synaptic plasticity, the AMPAR/NMDAR ratio was measured. AMPAR- and NMDAR-mediated currents elicited by LED stimulation were recorded in contralateral L5 neurons. A biocytin-filled L5 neuron and schematic are in Fig. 3*A*. The AMPAR/NMDAR ratio was not significantly different between groups (Student's *t* test: $P = 0.72$; Fig. 3*B* and *SI Appendix*, Table S5), indicating the increased AMPAR activity is matched by an increase in NMDAR activation in deprived L5 neurons targeted by the CC. We also measured the effects of ifenprodil, a GluN2B antagonist, on NMDAR-mediated callosal events. Ifenprodil sensitivity was doubled, indicating an increased proportion of the NMDAR-mediated current comprises GluN2B-containing receptors (Student's *t* test: $P = 0.01$; Fig. 3*C* and *SI Appendix*, Table S6). Decay kinetics of NMDAR-mediated events were not significantly altered between groups (*SI Appendix*, Fig. S5 and Tables S5 and S6). The increased prevalence of GluN2B-containing NMDARs may support CC strengthening.

Spontaneous Activity in Deprived S1BC L5 Neurons Has Larger Excitatory, but Not Inhibitory, Events. Unilateral whisker deprivation drives remarkable alterations in intact and deprived S1BC. Spontaneous activity may also be impacted by whisker deprivation, which could alter overall neural activity. Spontaneous excitatory postsynaptic currents (sEPSCs) and spontaneous inhibitory post synaptic currents (sIPSCs) were measured in sham and deprived L2/3 and L5 neurons. No change was detected in L2/3 sEPSC or sIPSC frequency or amplitude (sEPSC: Student's *t* test, amplitude $P = 0.16$, frequency $P = 0.35$, Fig. 4*A* and *SI Appendix*, Table S7; sIPSC: Student's *t* test, amplitude $P = 0.8$, frequency $P = 0.3$, Fig. 4*B* and *SI Appendix*, Table S7). L5 neurons experience an increase in sEPSC amplitude, but no change in frequency (Student's *t* test: amplitude $P = 0.01$, frequency $P = 0.6$; Fig. 4*C* and *SI Appendix*, Table S7), suggesting a postsynaptic mechanism. The sEPSC amplitudes did not increase multiplicatively (note the lack of overlap between the sham scaled and deprived lines) (Kolmogorov Smirnov Test: $P < 0.001$; Fig. 4*D*). The sIPSC frequency and amplitudes were not different between groups (Student's *t* test: amplitude $P = 0.24$, frequency $P = 0.87$; Fig. 4*E* and *SI Appendix*, Table S7). These results indicate that increased spontaneous excitatory amplitudes in deprived S1BC were not matched by spontaneous inhibitory events. There were no changes in sEPSC or sIPSC amplitudes or frequencies in intact L5

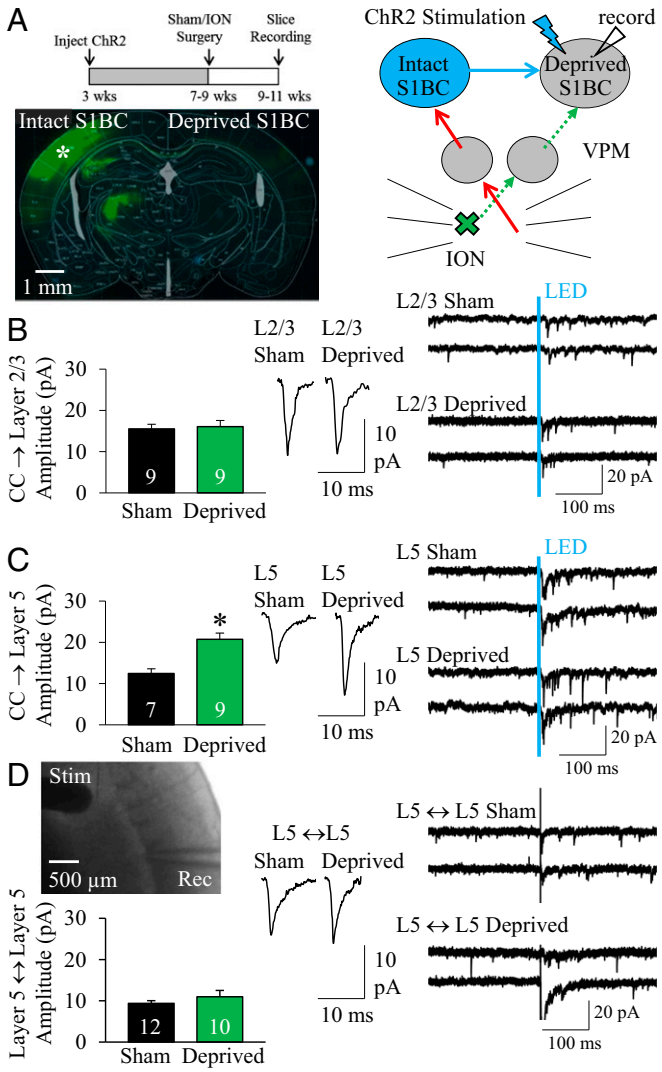

Fig. 2. Callosal projections from intact to deprived S1BC produce larger AMPAR-mediated events to L5 neurons after unilateral whisker deprivation. (*A*) Experimental design; asterisk is ChR2 injection site (green). (*B*) No change in light-evoked Sr-mEPSC amplitudes from intact to deprived L2/3. (*C*) Sr-mEPSCs are significantly larger to L5. (*D*) No change between local L5 to L5 electrically evoked Sr-mEPSC amplitudes. Average (*Center*) and representative (*Right*) traces are displayed in *B*–*D*. Bar graphs represent mean; error bars are SEM; * denotes statistical significance. *n*, number of cells.

neurons (*SI Appendix*, Fig. S4 and Table S8), indicating that the overall spontaneous activity experienced by L5 neurons in intact S1BC is not impacted by unilateral whisker denervation.

Increased Excitability Is Restricted to L5 Neurons in Deprived S1BC. L5 neurons in deprived S1BC have increased sEPSC amplitudes in addition to stronger callosally targeted synapses, which may contribute to altered intrinsic properties in deprived L5 neurons. The resting membrane potential (Vm), input resistance, and rheobase values were measured in S1BC L2/3 and L5 neurons. L2/3 cells did not demonstrate significant changes in Vm (Student's *t* test: $P = 0.1$; Fig. 5*A* and *SI Appendix*, Table S9), input resistance (Student's *t* test: $P = 0.8$, Fig. 5*B*) or rheobase values (Student's *t* test: $P = 0.6$; Fig. 5 *C* and *D* and *SI Appendix*, Table S9). L5 neurons in deprived S1BC had significantly depolarized Vm (Student's *t* test: $P = 0.01$; Fig. 5*E* and *SI Appendix*, Table S9), lower rheobase values (Student's *t* test: $P = 0.02$; Fig. 5 *G* and *H* and *SI Appendix*, Table S9), but no change in input resistance (Student's *t* test, $P = 0.79$; Fig. 5*F* and *SI Appendix*, Table S9). These results demonstrate that L5 neurons in deprived S1BC are more excitable. Intrinsic properties in L5 neurons of intact S1BC were also measured, but no changes were observed compared with sham (*SI Appendix*, Fig. S4*D* and Table S10). Deprived L5 neurons selectively experience a change in their intrinsic properties in response to altered circuit activity.

Potentiation of Callosal Inputs to L5 Principal Neurons Occludes LTP, Which Can Be Rescued After LTD. Little is known about what kind of plasticity the CC can undergo. A pairing protocol was used to elicit robust potentiation of callosal excitatory postsynaptic potentials in sham animals (Fig. 6*A*). This result indicates that callosal synapses to L5 principal cells remain plastic beyond the critical period, similar to other connections between L2/3 and L5 neurons (13) (protocols in *SI Appendix*, Fig. S6 *A*–*C*). The role of NMDARs in callosal LTP was tested with bath application of the NMDAR antagonist APV, or the GluN2B antagonist ifenprodil. Both drugs blocked LTP (*SI Appendix*, Fig. S6 *D* and *E*), indicating total NMDAR and specifically GluN2B containing NMDARs are required for callosal LTP.

In deprived S1BC, LTP could not be elicited at callosal inputs to L5 neurons (Fig. 6*A*). To determine the magnitude of callosal LTP capacity, multiple LTP inductions were performed, with 10-min recording intervals between each step. Callosal LTP in sham animals increased with each subsequent pairing (Fig. 6*B*), while intact to deprived LTP achieved only a minimal increase in potentiation with the third pairing (Fig. 6*B*). The values were statistically significant between the two groups at the second LTP pairing step

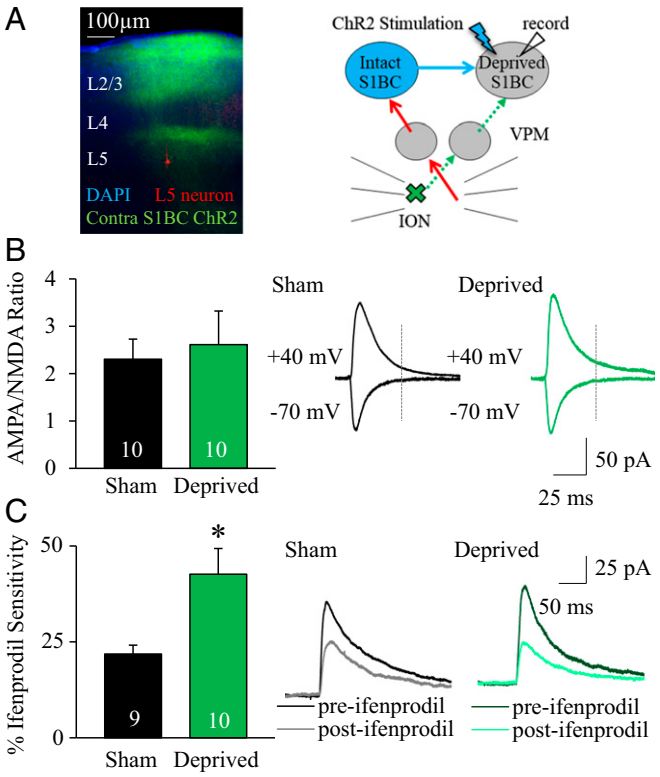

Fig. 3. NMDAR activity increases to match AMPAR in callosally targeted deprived L5 neurons, and indicates an increase in ifenprodil sensitivity. (*A*) Biocytin filled L5 principal neuron surrounded by callosal ChR2-YFP expressing terminals (*Left*); experimental schematic (*Right*). (*B*) No change in AMPAR/NMDAR ratio from intact to L5 neurons in deprived S1BC. (*C*) Deprived L5 neurons display increased ifenprodil sensitivity. Bar graphs represent mean; error bars are SEM; * denotes statistical significance. *n*, number of cells.

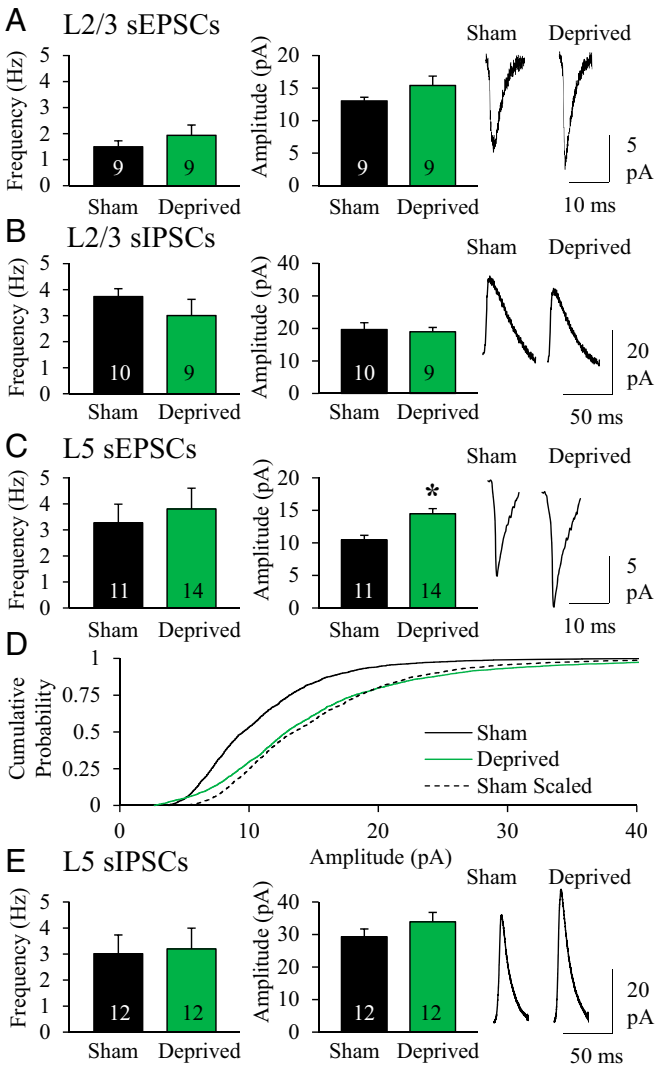

Fig. 4. Changes in spontaneous activity are restricted to sEPSCs in deprived L5 neurons. (*A* and *B*) The sEPSC and sIPSC amplitudes and frequency are not significantly altered in L2/3 (*Left* and *Center*); average traces (*Right*). (*C*) The sEPSC frequency is unchanged, but amplitude is larger in deprived L5 neurons. (*D*) The changes in sEPSC amplitude are not multiplicative. (*E*) The sIPSC frequency and amplitude are unchanged between groups. Bar graphs represent mean; error bars are SEM. *n*, number of cells.

[Student's *t* test: (*i*) $P = 0.07$, (*ii*) $P = 0.04$, (*iii*) $P = 0.07$]. Callosally evoked Sr-mEPSC amplitudes were larger in deprived S1BC L5 neurons, with a synaptic potentiation at a level similar to LTP magnitude in sham animals; thus it is likely that, in deprived S1BC, LTP has been occluded.

Callosal LTD was induced with a 1-Hz paired pulse protocol, and similar LTD was detected in L5 neurons from both groups (Fig. 6*C*). Interestingly, a pairing LTD protocol did not elicit LTD (*SI Appendix*, Fig. S6*F*), indicating that the CC may have unique requirements for LTD induction. To probe the synaptic floor, LTD was induced three times along the CC in sham and ION-transected animals. The first 10 min of LTD was significantly larger at callosal synapses from intact to deprived S1BC, but subsequent inductions produced equal LTD in both groups [Student's *t* test: (*i*) $P = 0.03$, (*ii*) $P = 0.6$, (*iii*) $P = 0.2$; Fig. 6*D*]. The CC has robust capability for both LTP and LTD in adults. Unilateral whisker denervation prevents callosal LTP from intact to deprived S1BC but does not affect LTD.

An LTP rescue experiment was performed by first inducing LTD and subsequently LTP in L5 neurons. This protocol elicited LTP in callosal synapses in both groups (Fig. 6*E*). LTP alone versus LTP rescue magnitudes were similar in sham (Student's *t* test: $P = 0.92$), but rescued LTP was larger than LTP alone in deprived L5 (Student's *t* test: $P = 0.02$). LTP can be induced at callosal synapses to deprived L5 neurons; thus this synapse maintains the necessary machinery to undergo LTP.

Discussion

Dramatic bilateral changes in cortical circuitry occur after unilateral whisker deprivation, summarized in *SI Appendix*, Fig. S6*G*. Intact whisker stimulation recruits a bilateral BOLD fMRI S1BC response. In the deprived S1BC, a stronger AMPAR-mediated postsynaptic response in L5, but not L2/3, neurons to callosal inputs was detected. Sham animals demonstrate remarkable capacity for LTP; however, with multiple inductions along the CC, LTP was not elicited in deprived L5 neurons. This indicates that these synapses have been maximally potentiated,

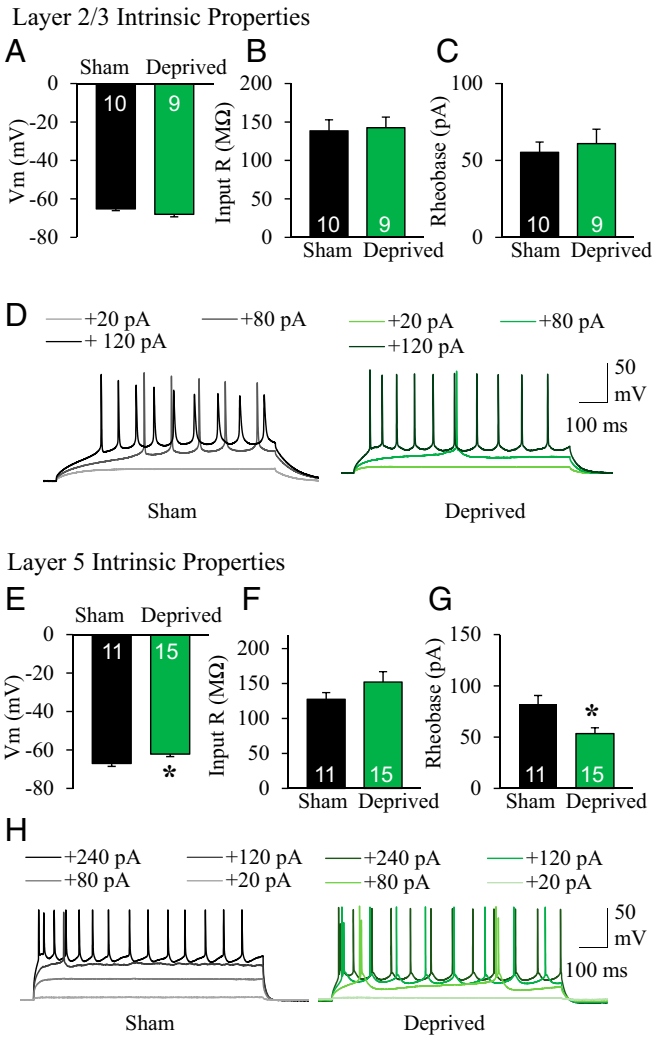

Fig. 5. Intrinsic properties of deprived L5 neurons demonstrate an increase in excitability; no change is detected in L2/3. Deprived L2/3 neurons have similar (*A*) Vm, (*B*) input resistance, and (*C*) rheobase values. (*D*) Representative traces. Deprived L5 neurons have (*E*) a higher Vm, (*F*) no change in input resistance, and (*G*) a lower rheobase value. (*H*) Representative traces. Bar graphs represent mean; error bars are SEM; * denotes statistical significance. *n*, number of cells.

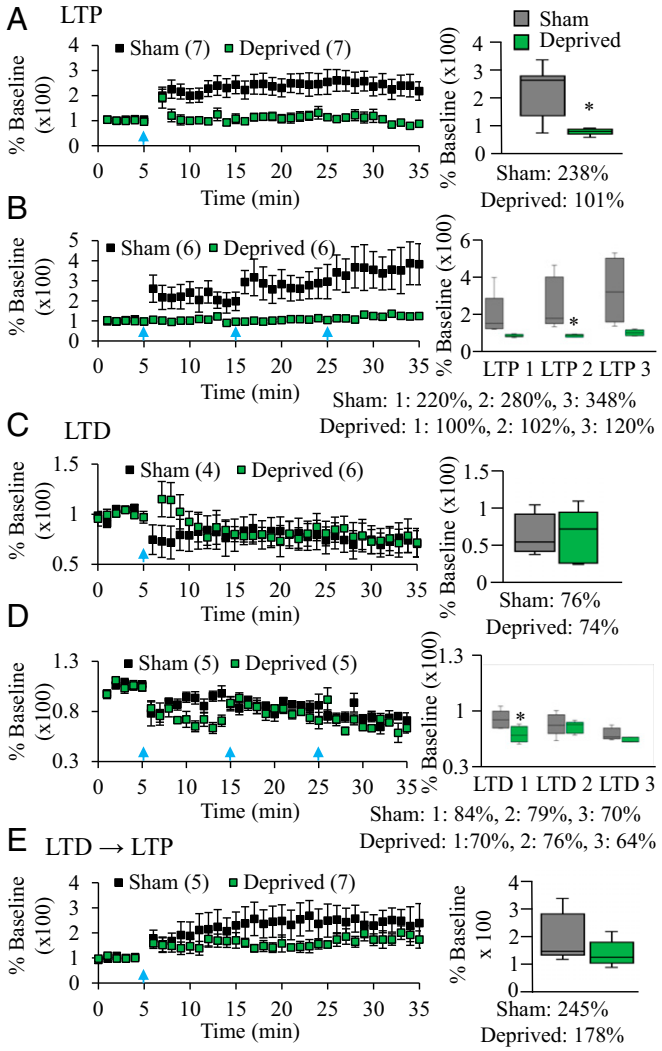

Fig. 6. Unilateral ION occludes callosal LTP from intact to deprived S1BC. LTD is similar between groups. (*A*) Robust callosal LTP to L5 neurons in sham is elicited; there is no LTP in deprived S1BC. (*B*) Multiple rounds of LTP induction produce progressively larger potentiation in sham, but deprived L5 neurons do not achieve LTP after multiple inductions. (*C*) LTD levels were equal between groups. (*D*) Multiple LTD inductions produced equal magnitudes between groups. (*E*) LTD induction before LTP protocol elicited LTP in the sham animals; deprived L5 LTP is rescued along the CC. Box plots represent mean; middle line is the median; error bars are minimum and maximum values; * denotes statistical significance.

which may be in response to the increase in AMPAR- and NMDAR-mediated event sizes at these synapses. Both sham and deprived L5 neurons equally achieved LTD; thus the synaptic floor was unchanged. Previous reports describing this type of dynamic range modification have been reported after training (14) or cocaine exposure (15). A dependence on NMDARs and an increase in mEPSC amplitudes were also described, consistent with our findings (15). Both of these reports demonstrated an increased capacity for LTD, which is not the case in our study. Either the possible modification range has been reduced with unilateral denervation or the robust LTD induction protocol that the CC requires may immediately bring the CC synapse to its floor; this would impair a more fine-tuned analysis of this pathway's LTD capacity. LTP and LTD mechanisms are at least partially mediated by AMPAR and NMDAR trafficking (16), and NMDAR subunit composition alters plasticity. GluN2B subunits are thought to underlie enhanced LTP in juvenile systems (17) and undergo a switch to NR2A in mature systems (18). Here we have described a requirement for NMDARs and, specifically, NR2B subunits to mediate callosal LTP in adult animals. The hypothesized increase in callosal GluN2B-containing NMDARs to deprived L5 neurons may further support potentiation; indeed, even with the increased NR2B activity LTP could not be induced, further arguing that LTP was occluded. These changes likely underlie the response recruitment in deprived S1BC detected with BOLD fMRI.

The doubling of AMPAR-mediated Sr-mEPSC amplitudes from callosal inputs corresponds to an unchanged AMPAR/NMDAR ratio and an increase in sensitivity to ifenprodil, a GluN2B antagonist. These measurements lead to the hypothesis that L5 neurons' callosal synapses have increased AMPARs, NMDARs, and GluN2B containing NMDARs. However, in the absence of biochemical proof of receptor distribution shifts, there are other factors which could also mediate the changes in deprived S1BC. For example, an increase in quantal size (19) or multivesicular release (20) could contribute to the increased amplitudes of glutamatergic events. In addition, it is known that NMDARs can be recruited to synapses in cases of high activity, resulting in synaptic spillover (21). Regardless of the mechanism, the increased glutamatergic responses of deprived L5 neurons to callosal inputs influence interhemispheric plasticity and bilateral cortical activity patterns.

The adaptations of deprived L5 neurons are likely a mixture of Hebbian and homeostatic mechanisms (22, 23). Deprived L5 neurons demonstrate increased excitability, and larger sEPSC amplitudes. This increase in size was not multiplicative, indicating this was not a strictly homeostatic response to whisker denervation. These larger events comprise callosal, lateral, and intracolumnar inputs. Postsynaptic modifications selectively occurred at callosal synapses onto L5 neurons, not callosal synapses to L2/3 cells, nor local L5 to L5 connections. The increased sEPSC amplitudes may indicate either that callosal synapses comprise the majority of inputs or that other inputs also increased their response size but were not recruited by local stimulation. The increased callosal drive to L5 neurons may be balanced by a reduction in feed-forward whisker stimuli. An increase in spontaneous event amplitudes and intrinsic excitability could signal a shift in the state of the deprived cortex to increase responsiveness to the intact whiskers.

Intact S1BC selectively targets L5 neurons in deprived S1BC after unilateral whisker deprivation. These results beg the question: Why L5? These neurons coordinate bilateral whisker information (5), and detect salient stimuli (24). L5 neurons are connected to widespread brain regions, including S2, M1, thalamus, and medial prefrontal cortex (25). L5 neurons are important for sensory detection and signal output. L5a and L5b may have different plasticity rules (26), but, for callosally targeted neurons in these experiments, both layers were represented equally and were not altered between groups. L5's capacity to evoke widespread changes, combined with bilateral stimuli integration, may explain why changes occur specifically in L5.

Bilateral S1BC BOLD fMRI responses to intact whisker stimulation were detected. These results are consistent with the requirement of the intact S1BC's presence to recruit deprived S1BC stimulus response (10). However, resting state fMRI (rs-fMRI) did not detect significant changes in S1BC bilateral connectivity. This may be due to the local restriction of plasticity to L5, or because anesthetic depth affects connectivity (27). Indeed, there is active discussion in the literature which has not yet reached a consensus on what circuit-level information rs-fMRI can extract about functional connectivity (28). Our model presents a useful tool for probing connectivity with rs-fMRI; however, higher-resolution scans with laminar discrimination or an awake preparation would be required to negate some of these confounds. Overall, the increase in evoked synaptic strength from

the intact to deprived S1BC may not translate to a visible change in connectivity.

Unilateral sensory deprivation can unmask previously subthreshold callosal inputs and increase receptive field size (29). Stroke reduces $GABA_B$-mediated callosal inhibition to perilesional areas, which does not change intrinsic properties but does unmask previously subthreshold inputs to L2/3 neurons in vivo (30). Despite the different injury model, the lack of change in L2/3 is consistent with our findings, and the hypothesis that a reduction in evoked interhemispheric inhibition elicits larger callosal responses may be applicable in our model, where, thus far, we have only demonstrated no change in spontaneous inhibitory events. Adult unilateral whisker deprivation triggers a recruitment of deprived S1BC to intact, ipsilateral whisker stimulation. The increased excitability combined with potentiated callosal synapses to deprived L5 cells could shift the state of deprived S1BC so it can be driven by intact S1BC. This recruitment may serve to increase the processing power of the intact whisker set, as seen in recruitment of deprived brain areas to process spared senses (31). Additionally, it may drive activity to prevent lateral plasticity, namely, blocking neighboring somatosensory areas from colonizing space in deprived S1BC (10). This lack of lateral plasticity could be beneficial: amputees with high levels of lateral reorganization have elevated incidence of phantom limb pain (32). However, brain reorganization after injury is critical for patients' rehabilitation (33).

This work may have relevance to the human brain. Unilateral stroke in somatomotor cortex demonstrates an initial increase in bilateral fMRI activity, which gradually returns to baseline in patients with optimal recovery (34). Similarly, shutting down deprived cortex with repetitive transcranial magnetic stimulation (rTMS) provides phantom limb pain relief in amputees (35). These effects might be mediated by the CC, but little is known about its role in interhemispheric plasticity. Here we have described the effects of unilateral whisker deprivation on specific receptors, synapses, and cell types which underlie alterations in callosal communication between bilateral somatosensory hemispheres. This circuit characterization lays the groundwork for understanding how unilateral perturbations may contribute to changes observed in humans using noninvasive imaging techniques. For example, if the phenomenon we describe is involved in beneficial recovery, interventions such as rTMS can be designed to speed up or otherwise enhance recovery by targeting deeper cortical layers (36). Understanding the circuit level changes may enhance our ability to aid patients' recovery from stroke or amputation by providing a guide for more specific, targeted interventions.

Materials and Methods

Animals. All procedures were approved by the National Institutes of Health Animal Care and Use Committee, facilities accredited by the Association for Assessment and Accreditation of Laboratory Animal Care. For complete methods referring to housing, stereotaxic injections of viruses, and ION transection surgery, please see *SI Appendix, Animal Procedures*.

Electrophysiology. All whole-cell slice electrophysiological recordings were performed 2 wk after ION transection or sham surgeries. For complete methods, please see *SI Appendix, Electrophysiology*.

fMRI. The fMRI experiments were performed under ketamine/xylazine anesthesia 2 wk after ION transection or sham surgeries in an 11.7-T MRI. Please see *SI Appendix, fMRI* for more details.

ACKNOWLEDGMENTS. Thanks go to H. K. Lee, C. McBain, R. Chittajallu, K. Pelkey, D. Picchioni, N. Bouraoud, K. Sheth, and K. Sharer. This research was supported (in part) by the Intramural Research Program of the NIH, National Institute of Neurological Disorders and Stroke.

1. Cao Y, Vikingstad EM, George KP, Johnson AF, Welch KMA (1999) Cortical language activation in stroke patients recovering from aphasia with functional MRI. *Stroke* 30: 2331–2340.
2. Kinsbourne M (1971) The minor cerebral hemisphere as a source of aphasic speech. *Arch Neurol* 25:302–306.
3. Grefkes C, et al. (2008) Cortical connectivity after subcortical stroke assessed with functional magnetic resonance imaging. *Ann Neurol* 63:236–246.
4. Rehme AK, Fink GR, von Cramon DY, Grefkes C (2011) The role of the contralesional motor cortex for motor recovery in the early days after stroke assessed with longitudinal FMRI. *Cereb Cortex* 21:756–768.
5. Shuler MG, Krupa DJ, Nicolelis MAL (2002) Integration of bilateral whisker stimuli in rats: Role of the whisker barrel cortices. *Cereb Cortex* 12:86–97.
6. Pietrasanta M, Restani L, Caleo M (2012) The corpus callosum and the visual cortex: Plasticity is a game for two. *Neural Plast* 2012:838672.
7. Kawaguchi Y (1992) Receptor subtypes involved in callosally-induced postsynaptic potentials in rat frontal agranular cortex in vitro. *Exp Brain Res* 88:33–40.
8. Petreanu L, Huber D, Sobczyk A, Svoboda K (2007) Channelrhodopsin-2-assisted circuit mapping of long-range callosal projections. *Nat Neurosci* 10:663–668.
9. Yu X, et al. (2012) Thalamocortical inputs show post-critical-period plasticity. *Neuron* 74:731–742.
10. Yu X, Koretsky AP (2014) Interhemispheric plasticity protects the deafferented somatosensory cortex from functional takeover after nerve injury. *Brain Connect* 4: 709–717.
11. Goda Y, Stevens CF (1994) Two components of transmitter release at a central synapse. *Proc Natl Acad Sci USA* 91:12942–12946.
12. Petrus E, et al. (2014) Crossmodal induction of thalamocortical potentiation leads to enhanced information processing in the auditory cortex. *Neuron* 81:664–673.
13. Huang S, et al. (2012) Pull-push neuromodulation of LTP and LTD enables bidirectional experience-induced synaptic scaling in visual cortex. *Neuron* 73:497–510.
14. Rioult-Pedotti MS, Friedman D, Donoghue JP (2000) Learning-induced LTP in neocortex. *Science* 290:533–536.
15. Ungless MA, Whistler JL, Malenka RC, Bonci A (2001) Single cocaine exposure in vivo induces long-term potentiation in dopamine neurons. *Nature* 411:583–587.
16. Malenka RC, Bear MF (2004) LTP and LTD: An embarrassment of riches. *Neuron* 44: 5–21.
17. Quinlan EM, Philpot BD, Huganir RL, Bear MF (1999) Rapid, experience-dependent expression of synaptic NMDA receptors in visual cortex in vivo. *Nat Neurosci* 2: 352–357.
18. Sheng M, Cummings J, Roldan LA, Jan YN, Jan LY (1994) Changing subunit composition of heteromeric NMDA receptors during development of rat cortex. *Nature* 368: 144–147.
19. Wilson NR, et al. (2005) Presynaptic regulation of quantal size by the vesicular glutamate transporter VGLUT1. *J Neurosci* 25:6221–6234.
20. Kombian SB, Hirasawa M, Mouginot D, Chen X, Pittman QJ (2000) Short-term potentiation of miniature excitatory synaptic currents causes excitation of supraoptic neurons. *J Neurophysiol* 83:2542–2553.
21. Oliet SHR, Papouin T (2014) Organization, control and function of extrasynaptic NMDA receptors. *Philos Trans R Soc Lond B Biol Sci* 369:20130601.
22. Bear MF, Cooper LN, Ebner FF (1987) A physiological basis for a theory of synapse modification. *Science* 237:42–48.
23. Turrigiano GG, Leslie KR, Desai NS, Rutherford LC, Nelson SB (1998) Activity-dependent scaling of quantal amplitude in neocortical neurons. *Nature* 391:892–896.
24. Shai AS, Anastassiou CA, Larkum ME, Koch C (2015) Physiology of layer 5 pyramidal neurons in mouse primary visual cortex: Coincidence detection through bursting. *PLoS Comput Biol* 11:e1004090.
25. DeNardo LA, Berns DS, DeLoach K, Luo L (2015) Connectivity of mouse somatosensory and prefrontal cortex examined with trans-synaptic tracing. *Nat Neurosci* 18:1687–1697.
26. Lefort S, Petersen CCH (2017) Layer-dependent short-term synaptic plasticity between excitatory neurons in the C2 barrel column of mouse primary somatosensory cortex. *Cereb Cortex* 27:3869–3878.
27. Grandjean J, Schroeter A, Batata I, Rudin M (2014) Optimization of anesthesia protocol for resting-state fMRI in mice based on differential effects of anesthetics on functional connectivity patterns. *Neuroimage* 102:838–847.
28. Leopold DA, Maier A (2012) Ongoing physiological processes in the cerebral cortex. *Neuroimage* 62:2190–2200.
29. Restani L, et al. (2009) Functional masking of deprived eye responses by callosal input during ocular dominance plasticity. *Neuron* 64:707–718.
30. Kokinovic B, Medini P (2018) Loss of $GABA_B$-mediated interhemispheric synaptic inhibition in stroke periphery. *J Physiol* 596:1949–1964.
31. Cohen LG, et al. (1997) Functional relevance of cross-modal plasticity in blind humans. *Nature* 389:180–183.
32. Flor H, Nikolajsen L, Staehelin Jensen T (2006) Phantom limb pain: A case of maladaptive CNS plasticity? *Nat Rev Neurosci* 7:873–881.
33. Chen R, Cohen LG, Hallett M (2002) Nervous system reorganization following injury. *Neuroscience* 111:761–773.
34. Grefkes C, Ward NS (2014) Cortical reorganization after stroke: How much and how functional? *Neuroscientist* 20:56–70.
35. Malavera A, Silva FA, Fregni F, Carrillo S, Garcia RG (2016) Repetitive transcranial magnetic stimulation for phantom limb pain in land mine victims: A double-blinded, randomized, sham-controlled trial. *J Pain* 17:911–918.
36. Gomez LJ, Goetz SM, Peterchev AV (2018) Design of transcranial magnetic stimulation coils with optimal trade-off between depth, focality, and energy. *J Neural Eng* 15:046033.